**SPEKTRA: Jurnal Fisika dan Aplikasinya**
Volume 9, Issue 2, August 2024
Homepage: doi.org/10.21009/SPEKTRA

DOI: doi.org/10.21009/SPEKTRA.092.02

# Exploring Weak Gravitational Lensing Effects by a Regular Black Hole

A. K. Durrani*, H. S. Ramadhan

*Department Fisika, FMIPA, Universitas Indonesia, Depok, 16424, Indonesia*

*Corresponding Author Email: afrasiab.khan@ui.ac.id

**Received**: 9 June 2024
**Revised**: 2 July 2024
**Accepted**: 4 July 2024
**Online**: 15 July 2024
**Published**: 30 August 2024

**SPEKTRA**: Jurnal Fisika dan Aplikasinya
p-ISSN: 2541-3384
e-ISSN: 2541-3392

## ABSTRACT

Gravitational lensing is one of the physical consequences of Einstein's general theory of relativity, which has been observationally confirmed. This work aims to study the weak gravitational lensing scenario where the lens is a spherically symmetric, charged-nonsingular black hole that asymptotically behaves as the Reissner-Nordström (RN). The difference exists in the higher-order expansion. Therefore, the metric function of the regular charged black hole is expanded up to the fourth order, and the deflection angle is calculated. The thin lens equation is used, leading to five images: two imaginary and three real images. The exact positions of the images and magnification properties are calculated by providing the physical parameters such as mass, charge, and distances. Our calculation shows that the third image position shifted away from the optical axis. The formalism is applied to the case of a supermassive black hole located at the center of our galaxy with the assumption that it has an electric charge.

**Keywords**: gravitational lensing, regular charged black hole, deflection angle, image positions, magnification

## INTRODUCTION

GR offers profound insights into the nature of black holes [1], with gravitational lensing serving as a potent tool for probing their characteristics and verifying Einstein's theory. Over the years, numerous studies on gravitational lensing have been conducted, including recent works by Fritteli, Kling, and Newman [2], by Virbhadra and Ellis [3], and Bozza et al. [4]. In [5], Fernando and Roberts studied weak gravitational lensing by a charged black hole, namely, the Reissner-Nordström Black Hole. They calculated the deflection angle and the exact image positions using thin lens equation. In recent years, a particular focus has been directed towards

understanding weak gravitational lensing by regular charged black holes. These black holes are characterized by their electric charge and absence of singularities at their centers. The study of weak gravitational lensing by regular charged black holes not only contributes to our comprehension of astrophysical phenomena but also has implications for testing and refining gravitational theories. Over the past two decades, a notable area of research has centered on exploring the interiors of black holes. This inquiry has led to the publication of various examples of regular exact black hole solutions in the literature, providing compelling evidence that black holes do not always culminate in singularities [6], [7], [8], [9]. Bardeen [10] laid the theoretical foundation for this field of study by proposing the first regular black hole model (see also Refs. [11], [12]). The Bardeen model is a black hole that conforms to the weak energy condition and has been crucial in further explorations into spacetime singularities. Later, more regular black hole models were suggested [11], [12], [13], [14], [15], [16], [17].

Recent advancements have explored the implications of modified gravity theories on black hole lensing, such as the work by Izmailov et al. [18] on modified gravity black hole lensing observables. The lensing effects of loop quantum gravity black holes have also been studied, providing new insights into quantum gravity corrections [19]. Additionally, gravitational lensing by string theory black holes has revealed unique characteristics influenced by stringy effects [20]. Furthermore, Liu et al. [21] investigated the lensing effects in the context of non-minimal Einstein-Yang-Mills black holes, highlighting the impact of different gravitational theories on lensing observables.

This research aims to investigate weak gravitational lensing by a regular charged black hole. The deflection angles and image positions of light rays near these exotic objects are calculated. First, a concise overview of the fundamental principles behind gravitational lensing of an object with spherical symmetry is provided. Following this, the features of regular charged black holes are discussed. Subsequently, the deflection angle by a regular charged black hole and a Reissner-Nordström black hole is calculated. Finally, the images formed by a general regular black hole metric are discussed and calculated, and the findings are summarized.

## GRAVITATIONAL LENSING AROUND A SPHERICALLY-SYMMETRIC OBJECT

The line element around a static, spherically-symmetric black hole is given by

$$ds^2 = B(r)\,dt^2 - A(r)\,dr^2 - r^2(d\theta^2 + \sin^2\theta d\varphi), \tag{1}$$

where $B(r)$ and $A(r)$ are the metric functions. By solving the null geodesics equation, the equation for light trajectory:

$$\frac{A(r)}{r^4}\left(\frac{dr}{d\varphi}\right)^2 + \frac{1}{r^2} - \frac{1}{b^2 B(r)} = 0, \tag{2}$$

illustrated in FIGURE 1 can be found. At the closest distance, $r_0$, $dr/d\varphi$ vanishes. So the relation between impact parameter $b$ and distance of closest approach $r_0$ can be obtain as

$$b = r_0\left(B(r_0)\right)^{-\frac{1}{2}}. \tag{3}$$

Relative to an inertial observer at infinity, the quantity $r_0$ is the distance of closest approach to the center of the black hole, while the impact parameter $b$ is the perpendicular distance from the black hole's center to the asymptotic tangent line to the light ray converging at the observer.

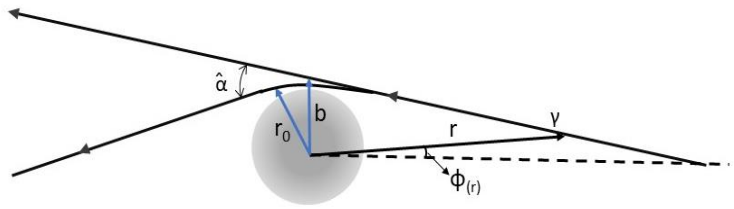


**FIGURE 1.** The figure illustrates deflection of light by a static spherically symmetric black hole, the quantities $\boldsymbol{b}$, $\boldsymbol{r_0}$, which are defined in the text. However, $\boldsymbol{\varphi_{(r)}}$ represents the azimuthal angle of the photon.

Defining $\gamma = |\phi_{(r)} - \phi_\infty|$, with $\phi_\infty = \phi(\, r \to \infty\,)$, from the FIGURE 1, the total angle of deflection $\hat{\alpha}$ can be obtained as,

$$\hat{\alpha} = 2\gamma - \pi,$$

$$\hat{\alpha} = 2\int_{r_0}^{\infty} A^{\frac{1}{2}}(r)\left[\left(\frac{r}{r_0}\right)^2\left(\frac{B(r_0)}{B(r)}\right) - 1\right]^{-\frac{1}{2}}\frac{dr}{r} - \pi. \tag{4}$$

By deflecting light ray, black hole can act as a lens. The geometrical configuration of the lensing is illustrated in FIGURE 2.

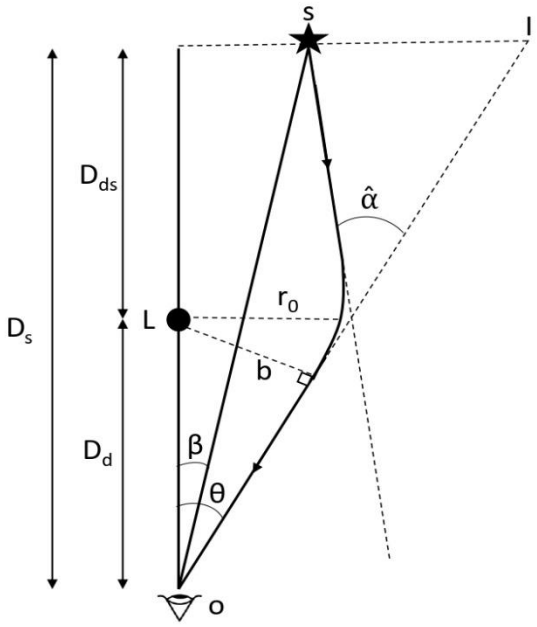


**FIGURE 2.** The geometry of lensing. Here, $\boldsymbol{S}$, $\boldsymbol{L}$, and $\boldsymbol{I}$ represents the source position, the lens, and the image position, respectively. The angular separation of the source from the lens is given by $\boldsymbol{\beta}$, while the image is given by $\boldsymbol{\theta}$. $\hat{\boldsymbol{\alpha}}$ is given by the Einstein bending angle derived above. $\boldsymbol{D_{ds}}$ represents the lens-source distance, $\boldsymbol{D_d}$ represents the observer-lens distance and $\boldsymbol{D_s}$ shows the source-observer distance.

The geometrical relations between the lensing angles (in the thin lens approximation) can be obtained from the FIGURE 2 and can be expressed as,

$$\beta = \theta - \hat{\alpha}\,\frac{Dds}{Ds}\,, \tag{5}$$

when the impact parameter is much greater than the event horizon, $b \gg r^{+}$. The quantities $\theta$ and $\beta$ are the angular positions of the image and the unlensed source relative to the optical axis, respectively. The magnification $\mu$ of the images for the thin lens approximation is given by the inverse of the Jacobian [22] evaluated at the position of the image and is given as,

$$\mu = \frac{d\theta}{d\beta}\frac{\theta}{\beta}. \tag{6}$$

## REGULAR CHARGED BLACK HOLE

Regular black hole is a black hole whose core is completely regular, devoid of any singularity [23]. The metric in general is given by $B(r) = A^{-1}(r) = f(r) \equiv 1 - \frac{2m(r)}{r}$. Here, $m(r)$ is the mass function and can be expressed as,

$$m(r) = \frac{\sigma_{(r)}}{\sigma_{\infty}}\,M, \tag{7}$$

where $\sigma(r)$ is distribution function which satisfies $\sigma(r) > 0$, $\sigma'(r) > 0$ for $r \geq 0$.

Further, if $r \to 0$ the term $\sigma(r)\,/\,r \to 0$, similarly, for $r \to \infty$ the distribution function can be shown as $\sigma_{\infty} = \sigma(r \to \infty)$, which represents its normalization factor. Few distribution functions have been constructed and are given in [22]. One of the distribution function is,

$$o(r) = \left(\frac{\frac{Q^2}{Mr}}{e^{\frac{Q^2}{Mr}} - 1}\right), \tag{8}$$

the metric then becomes,

$$f(r) = 1 - \frac{2M}{r}\left(\frac{\frac{Q^2}{Mr}}{e^{\frac{Q^2}{Mr}} - 1}\right). \tag{9}$$

The event horizon can be determined by $f(r) = 0$. The extremal charge can be determined numerically $Q_c \cong 1.1381\,M$, and the corresponding extremal horizon location is at $r_h \cong 0.81281\,M$.

## DEFLECTION ANGLE BY A REGULAR CHARGED BLACK HOLE

The corresponding deflection angle for the regular black hole in EQUATION (9) is given by expanding the integrands in EQUATION (4) up to the fourth order of $(1/r)$.

$$\left[\left(\frac{r}{r}\right)^2\left(\frac{B(r_0)}{B(r)} - 1\right)\right]^{-\frac{1}{2}}$$

$$\approx \frac{r^2}{r_0{}^2}+\frac{2Mr}{r_0{}^2}-\frac{2Mr^2}{r_0{}^3}+\frac{Q^2r^2}{r_0{}^4}-\frac{Q^2}{r_0{}^2}+\frac{4M^2}{r_0{}^2}-\frac{4M^2r}{r_0{}^3}+\frac{8M^3}{r_0{}^2 r}-\frac{8M^3}{r_0{}^3}+\frac{Q^4}{6M\,r\,r_0{}^2}-\frac{Q^4\,r^2}{6M\,r_0{}^5}$$
$$+\frac{2M\,Q^2}{r_0{}^3}-\frac{2M\,Q^2}{r_0{}^2\,r}+\frac{2M\,Q^2\,r}{r_0{}^4}-\frac{2M\,Q^2\,r}{r_0{}^2\,r}+\frac{16\,M^4}{r_0{}^2\,r^2}-\frac{16\,M^4}{r_0{}^3\,r}+\frac{4\,M^2Q^2}{r_0{}^4}+\frac{8\,M^2Q^2}{r_0{}^3\,r}-\frac{12\,M^2Q^2}{r_0{}^2\,r^2}$$
$$-\frac{Q^4r^2}{6\,r_0{}^5\,M}-\frac{Q^4r}{3\,r_0{}^5}-\frac{Q^4}{r_0{}^4}-\frac{Q^4}{3\,r_0{}^3\,r}+\frac{Q^4}{6\,r_0{}^2Mr}+\frac{5\,Q^4}{3\,r_0{}^2\,r^2}-1\,. \tag{10}$$

The deflection angle can then be written as,

$$\hat{\alpha}\approx\frac{4\,M}{r_0}+\frac{4\,M^2}{r_0{}^2}\left(\frac{15\pi}{16}-1\right)-\frac{3\,Q^2\pi}{4\,r_0{}^2}+\frac{M^3}{r_0{}^3}\left(-\frac{15\pi}{2}+36\right)+\frac{M\,Q^2}{r_0{}^3}\left(\frac{3\pi}{2}-14\right)$$
$$+\frac{M^4}{r_0{}^4}\left(\frac{3465\pi}{64}-\frac{434}{3}\right)+\frac{M^2Q^2}{r_0{}^4}\left(-\frac{825\pi}{32}+50\right)+\frac{Q^4}{r_0{}^4}\left(-\frac{127\pi}{64}-\frac{5}{3}\right)+\frac{4\,Q^4}{9\,r_0{}^3M}\,. \tag{11}$$

By inserting EQUATION (11) into EQUATION (5), a polynomial equation of fifth-order can be constructed as

$$A_1\theta^5+A_2\theta^4+A_3\theta^3+A_4\theta^2+A_5\theta^1+A_6=0, \tag{12}$$

where $r_0\equiv\theta D_d$, and

$$A_1\equiv 1,$$
$$A_2\equiv-\beta,$$
$$A_3\equiv-4\,M\frac{D_{ds}}{D_d\,D_s},$$
$$A_4\equiv\left(4\,M^2\left(\frac{15\pi}{16}-1\right)-\frac{3\,Q^2\pi}{4}\right)\frac{D_{ds}}{D_d{}^2D_s},$$
$$A_5\equiv\left(M^3\left(-\frac{15\pi}{2}+36\right)+M\,Q^2\left(\frac{3\pi}{2}-14\right)+\frac{4\,Q^4}{9\,M}\right)\frac{D_{ds}}{D_d{}^3D_s}, \tag{13}$$
$$A_6\equiv\left(M^4\left(\frac{3465\pi}{64}-\frac{434}{3}\right)+M^2Q^2\left(-\frac{825\pi}{32}+50\right)+Q^4\left(-\frac{127\pi}{64}-\frac{5}{3}\right)\right)\frac{D_{ds}}{D_d{}^4D_s},$$

EQUATION (12) yields a total of five roots, only three of which are real. In FIGURE 3, the deflection angles $\hat{\alpha}(r_0)$ were plotted for both the regular and RN black holes as functions of the closest approach $(r_0)$, which illustrates that at low charge, there exists a notable difference between the deflection angles of both models. The deflection angle of the regular black hole is greater than RN for the parametric values: $M=1$ and $Q=1/\sqrt{2}$.

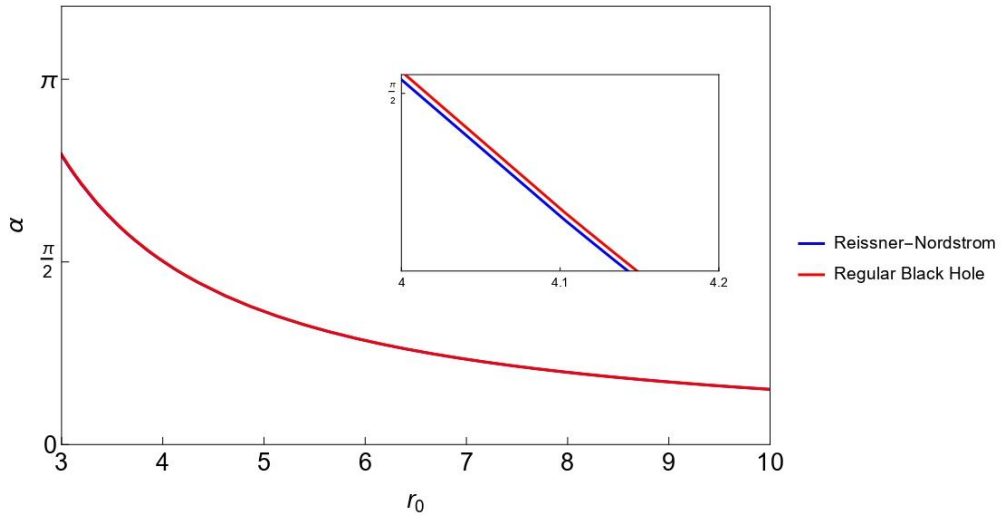


**FIGURE 3.** The deflection $\hat{\boldsymbol{\alpha}}(\boldsymbol{r_0})$ for both the regular and the RN black holes is plotted against distance of closest approach $\boldsymbol{r_0}$, with the parametric values as $\boldsymbol{M = 1}$ and $\boldsymbol{Q = 1/\sqrt{2}}$.

## CALCULATION FOR THE IMAGES BY A GENERAL REGULAR BLACK HOLE METRIC

In this section, the corresponding lensing images and magnification are found using the following numerical values: $M = 2.8 \times 10^6\, M_\odot$, $D_{ds}/D_s = 1/2$, $D_d = 8.5$ kpc, and $Q^2 = M^2/2$. This models the supermassive black hole located in the center of our galaxy to be a regular one, taking into account the possibility that it is electrically charged. The image positions $\theta$ for different values of the source position ($\beta$) are given in TABLE 1. We can see that the first two images' positions are much bigger than the third one.

**TABLE 1.** Image positions ($\theta$) for different values of source position ($\beta$). The angles are given by arcseconds.

| Regular Black Hole | | | | Reissner-Nordström Black Hole | | |
|---|---|---|---|---|---|---|
| $\beta$ | $\theta_1$ | $\theta_2$ | $\theta_3$ | $\theta_1$ | $\theta_2$ | $\theta_3$ |
| $10^{-4}$ | 1.15587 | -1.15577 | $-4.975311\times10^{-6}$ | 1.15587 | -1.15577 | $-4.919013\times10^{-6}$ |
| $10^{-3}$ | 1.15632 | -1.15532 | $-4.975311\times10^{-6}$ | 1.15632 | -1.15532 | $-4.919013\times10^{-6}$ |
| $10^{-2}$ | 1.16083 | -1.15083 | $-4.975311\times10^{-6}$ | 1.16083 | -1.15083 | $-4.919013\times10^{-6}$ |
| $10^{-1}$ | 1.20690 | -1.1069 | $-4.975312\times10^{-6}$ | 1.20690 | -1.1069 | $-4.919014\times10^{-6}$ |
| 1 | 1.75933 | -0.759329 | $-4.975322\times10^{-6}$ | 1.75933 | -0.759329 | $-4.919024\times10^{-6}$ |
| 2 | 2.52837 | -0.528367 | $-4.975333\times10^{-6}$ | 2.52837 | -0.528367 | $-4.919035\times10^{-6}$ |
| 3 | 3.39365 | -0.393647 | $-4.975344\times10^{-6}$ | 3.39365 | -0.393647 | $-4.919045\times10^{-6}$ |
| 4 | 4.30996 | -0.309949 | $-4.975355\times10^{-6}$ | 4.30996 | -0.309949 | $-4.919056\times10^{-6}$ |
| 5 | 5.25425 | -0.254249 | $-4.975366\times10^{-6}$ | 5.25425 | -0.254249 | $-4.919067\times10^{-6}$ |

The images produced by regular charged black hole exhibit magnification features, which may be described by the following expression:

$$\mu = \frac{\theta}{\beta}\frac{d\theta}{d\beta} = -\frac{\theta_5}{A_2\,(5\,A_1\,\theta^4 + 4A_2\,\theta^3 + 3\,A_3\,\theta^2 + 2\,A_4\,\theta + A_5)}\,. \qquad (14)$$

The magnification properties have been computed for various source positions and are shown in TABLE 2. The magnification diminishes rapidly as $\beta$ rises. Therefore, the images located

on the outermost part are more probable to be seen compared to the rest. The third image exhibits much lower brightness in comparison to the source, hence causing challenges for observations.

**TABLE 2.** Magnification of the corresponding images for different values of source position ($\beta$).

| Regular Black Hole | | | | Reissner-Nordström Black Hole | | |
|---|---|---|---|---|---|---|
| $\beta$ | $\theta_1$ | $\theta_2$ | $\theta_3$ | $\theta_1$ | $\theta_2$ | $\theta_3$ |
| $10^{-4}$ | 5779.6 | -5778.6 | $5.46009\times10^{-13}$ | 5779.6 | -5778.6 | $5.33164\times10^{-13}$ |
| $10^{-3}$ | 578.41 | -577.41 | $5.46009\times10^{-14}$ | 578.41 | -577.41 | $5.33164\times10^{-14}$ |
| $10^{-2}$ | 58.2926 | -57.2926 | $5.46009\times10^{-15}$ | 58.2926 | -57.2926 | $5.33164\times10^{-15}$ |
| $10^{-1}$ | 6.29531 | -5.29531 | $5.46009\times10^{-16}$ | 6.29531 | -5.29531 | $5.33165\times10^{-16}$ |
| 1 | 1.22892 | -0.228925 | $5.46017\times10^{-17}$ | 1.22892 | -0.228925 | $5.33172\times10^{-17}$ |
| 2 | 1.04567 | -0.0456654 | $2.730125\times10^{-17}$ | 1.04567 | -0.0456654 | $2.66589\times10^{-17}$ |
| 3 | 1.01364 | -0.0136386 | $1.820110\times10^{-17}$ | 1.01364 | -0.0136386 | $1.77729\times10^{-17}$ |
| 4 | 1.0052 | -0.0051989 | $1.365103\times10^{-17}$ | 1.0052 | -0.0051989 | $1.33299\times10^{-17}$ |
| 5 | 1.00235 | -0.0023471 | $1.092099\times10^{-17}$ | 1.00235 | -0.0023471 | $1.06641\times10^{-17}$ |

## CONCLUSION

The weak gravitational lensing of a regular black hole proposed by Balart and Vagenas [22] was studied, and its optical observables were computed. The exact position of the images was determined, and it was observed that the position of the third image is shifted away from the optical axis on the opposite side of the source position. The first two images are bright, and their magnification diminishes rapidly as $\beta$ rises. Although the third image presents a challenge for observations due to its extremely low luminance in relation to the source. The supermassive black hole in the center of our galaxy was modeled as a regular one. Therefore, future astronomical observations of this black hole may use this study's findings as a reference.

However, since black holes possess a strong gravitational field, it is certainly worthwhile to investigate the phenomenon of lensing caused by a regular charged black hole. By employing the full lens equation, large bending angles can be accounted for. Virbhadra et al. [3] used the full lens equation to identify "relativistic images" for the Schwarzschild black hole. Bozza [24] presented an analytical method to find the deflection angle and other strong lensing observables for different models. There was another attempt by Tsukamoto [25] to calculate the deflection angle in the strong deflection limit using different approach than the one used by Bozza in [24]. One can utilize the above-mentioned approach to calculate the deflection angle and other observables for this regular black hole as given in EQUATION 9. This research is intended to be published in the future.

## ACKNOWLEDGEMENTS

Fathoni Shidik and Hassan Moin Ud Din are thanked for their enlightening discussions. This research is supported by the Hibah Riset FMIPA UI No. PKS-026/UN2.F3.D/PPM.00.02 /2023.

## REFERENCES


[1] S. Chandrasekhar, *The Mathematical Theory of Black Holes*. New York: Oxford University Press, 1998.

[2] T. P. Kling and E. T. Newman, "Spacetime perspective of Schwarzschild lensing," *Physical Review D - Particles, Fields, Gravitation and Cosmology*, vol. 61, no. 6, 2000, doi: 10.1103/PHYSREVD.61.064021.

[3] K. S. Virbhadra and G. F. R. Ellis, "Schwarzschild black hole lensing," *Physical Review D - Particles, Fields, Gravitation and Cosmology*, vol. 62, no. 8, pp. 1–8, Oct. 2000, doi: 10.1103/PHYSREVD.62.084003.

[4] V. Bozza, S. Capozziello, G. Iovane, and G. Scarpetta, "Strong field limit of black hole gravitational lensing," *Gen Relativ Gravit*, vol. 33, no. 9, pp. 1535–1548, 2001, doi: 10.1023/A:1012292927358.

[5] S. Fernando and S. Roberts, "Gravitational lensing by charged black holes," *Gen Relativ Gravit*, vol. 34, no. 8, pp. 1221–1230, 2002, doi: 10.1023/A:1019726501344.

[6] E. Ayón-Beato and A. García, "Regular black hole in general relativity coupled to nonlinear electrodynamics," *Phys Rev Lett*, vol. 80, no. 23, pp. 5056–5059, 1998, doi: 10.1103/PHYSREVLETT.80.5056.

[7] E. Ayón-Beato and A. García, "New regular black hole solution from nonlinear electrodynamics," *Physics Letters B*, 1999. Accessed: Jun. 15, 2024, doi: 10.1016/S0370-2693(99)01038-2.

[8] E. Ayón-Beato and A. Garcia, "Non-Singular Charged Black Hole Solution for Non-Linear Source," *Gen Relativ Gravit*, vol. 31, no. 5, pp. 629–633, May 1999, doi: 10.1023/A:1026640911319.

[9] E. Ayón-Beato and A. García, "The Bardeen model as a nonlinear magnetic monopole," *Physics Letters B*, 2000. Accessed: Jun. 15, 2024, doi: 10.1016/S0370-2693(00)01125-4

[10] S. Orzuev, F. Atamurotov, A. Abdujabbarov, and A. Abduvokhidov, "Weak gravitational lensing of black hole from T-duality in plasma," *New Astronomy*, vol. 105, Jan. 2024, doi: 10.1016/j.newast.2023.102104.

[11] A. Borde, "Open and closed universes, initial singularities, and inflation," *Physical Review D*, vol. 50, no. 6, pp. 3692–3702, 1994, doi: 10.1103/PHYSREVD.50.3692.

[12] A. Borde, "Regular black holes and topology change," *Physical Review D - Particles, Fields, Gravitation and Cosmology*, vol. 55, no. 12, pp. 7615–7617, 1997, doi: 10.1103/PHYSREVD.55.7615.

[13] V. P. Frolov, "Information loss problem and a `black hole' model with a closed apparent horizon," *Journal of High Energy Physics*, 2014, doi: 10.1007/JHEP05(2014)049.

[14] V. P. Frolov, "Remarks on non-singular black holes," *EPJ Web of Conferences*, Aug. 2017, doi: 10.1051/epjconf/201816801001.

[15] R. Carballo-Rubio, F. Di Filippo, S. Liberati, C. Pacilio, and M. Visser, "On the viability of regular black holes," *Journal of High Energy Physics*, May 2018, doi: 10.1007/JHEP07(2018)023.

[16] V. P. Frolov, "Notes on non-singular models of black holes," *Physical Review D*, Sep. 2016, doi: 10.1103/PhysRevD.94.104056.

[17] V. P. Frolov and A. Zelnikov, "Quantum radiation from an evaporating non-singular black hole," *Physical Review D*, Apr. 2017, doi: 10.1103/PhysRevD.95.124028.

[18] R. Izmailov, R. Karimov, and E. R. Zhdanov, "Modified gravity black hole lensing observables in weak and strong field of gravity," *Monthly Notices of the Royal Astronomical Society*, 2018, doi: 10.1093/MNRAS/STY3350.

[19] S. Sahu, K. Lochan, and D. Narasimha, "Gravitational lensing by a black hole in effective loop quantum gravity," *Physical Review D*, 2015, doi: 10.1103/PhysRevD.91.063001.

[20] A. Bhadra, "Gravitational lensing by a charged black hole of string theory," *Physical Review D*, 2003, doi: 10.1103/PhysRevD.67.103009.

[21] F.-Y. Liu, Y.-F. Mai, W. Wu, and Y. Xie, "Probing a regular non-minimal Einstein-Yang-Mills black hole with gravitational lensings," *Physics Letters B*, 2019, doi: 10.1016/J.PHYSLETB.2019.06.052.
[22] L. Balart and E. C. Vagenas, "Bardeen regular black hole with an electric source," *Physical Review D* - Particles, Fields, Gravitation and Cosmology, vol. 90, no. 12, p. 124045, Dec. 2014, doi: 10.1103/PHYSREVD.90.124045.
[23] J. P. S. Lemos and V. T. Zanchin, "Regular black holes: Electrically charged solutions, Reissner-Nordström outside a deSitter core," *Physical Review D - Particles, Fields, Gravitation and Cosmology*, vol. 83, no. 12, Jun. 2011, doi: 10.1103/PHYSREVD.83.124005.
[24] V. Bozza, "Gravitational lensing in the strong field limit," *Physical Review D - Particles, Fields, Gravitation and Cosmology*, vol. 66, no. 10, Nov. 2002, doi: 10.1103/PHYSREVD.66.103001.
[25] N. Tsukamoto, "Deflection angle in the strong deflection limit in a general asymptotically flat, static, spherically symmetric spacetime," *Physical Review D*, vol. 95, no. 6, Mar. 2017, doi: 10.1103/PHYSREVD.95.064035.